An approach to generating two zones of silence with application to personal sound systems

M. A. Poletti
Callaghan Innovation, P.O. Box 31-310, Lower Hutt, New Zealand

F. M. Fazi
Institute of Sound and Vibration Research, University of Southampton, SO17 1BJ, United Kingdom

Upload date January 14th, 2015

Running title: Zones of silence

Abstract:

An application of current interest in sound reproduction systems is the creation of multizone sound fields which produce multiple independent sound fields for multiple listeners. The challenge in producing such sound fields is the avoidance of interference between sound zones, which is dependent on the geometry of the zone and the direction of arrival of the desired sound fields. This paper provides a theoretical basis for the generation of two zones based on the creation of sound fields with nulls and the positioning of those nulls at arbitrary positions. The nulls are created by suppressing low-order mode terms in the sound field expansion. Simulations are presented for the 2D case which show that suppression of interference is possible across a broad frequency audio range.

PACS numbers 43.60.Fg, 43.38.Md, 43.60.Tj

I. INTRODUCTION

A problem of current interest is the creation of multiple sound zones, which allow two or more listeners to hear different audio signals at different positions in space. The use of headphones allows individual listening, but these become uncomfortable after extended use, and alternative methods have been investigated, using loudspeaker arrays to create multiple personal sound zones [1–6]. Commonly two zones are considered, but some attempts have been made to produce three or more zones [6,7].

Optimum methods have been considered based on controlling the space-averaged potential energy density. One method considered brightness maximization with a power constraint and a second maximized the ratio of the energy density between the two regions[2,8–10]. The maximization of the difference in energy between regions was also considered [11], where it was shown that maximizing the difference can be more robust than maximizing the ratio while maintaining a desired energy level.

These energy-based methods do not control the phase of the reproduced sound field, and hence the direction of propagation. Control of the energy and the direction of propagation can be provided by direct pressure matching [7,12], by modal control [5,6,13], by the control of acoustic intensity [3] or by combining optimum contrast methods with pressure matching [14–17].

Methods that exploit sparsity have also been applied to reduce the complexity of sound field reproduction: pressure matching has been combined with a Lasso approach to reduce the number of loudspeakers[12]. Multizone reproduction in reverberant rooms has been considered where a reduction in complexity is achieved by modeling the reverberant response as a sparse set of plane waves[18].

Solutions to the N-zone problem must provide N sound fields in which the n-th field must have regions of silence at the position of the other (N–1) zones. For sound zones which are sufficiently separate in space, and for certain directions of propagation, standard beam-forming techniques will be sufficient to allow sound to be directed between silent zones to illuminate a desired target zone [1,19,20]. However, if the direction of sound propagation is along the line through the centre of two zones, the sound must travel through the desired zone and then avoid the silent zone. This is possible if the silent zone is physically isolated by a sound barrier, in which case the silent zone is a separate enclosure and sound diffracts around the enclosure boundary. In the absence of an enclosure, however, sound must avoid the silent zone without the aid of a physical barrier. This counter-intuitive objective may seem difficult to achieve. Nevertheless, numerical solutions have shown that wave fronts can avoid an in-line or close to in-line silent zone [7,17].

This paper attempts to provide a physical explanation for the effect. An approach to the multi-zone problem is considered in which a sound field is developed that is a solution to the wave equation in cylindrical harmonics and that produces a single zone of silence (ZOS). If the low-order modes of the cylindrical expansion are suppressed, a null is formed, due to the high-pass nature of the Bessel functions at low values of the argument. A second field can then be generated which will produce a desired field in the null region without interference, and avoiding the need to suppress interference terms[13]. Similarly, suppressing the low order terms of the second field will produce a null in which the first field can be heard without interference. This approach demonstrates that there is a sound physical basis for the generation of two independent sound zones with no inter-zone interference. The paper considers the free-field, 2D case for simplicity. However the results also extend to the 3D case.

The structure of this paper is as follows. In section II the theoretical basis for the creation of a single, frequency-independent ZOS is presented. Section III considers the creation of a zone at an arbitrary position. Section IV discusses the generation of a two-zone sound field using a circular array of sources and presents simulation results.

II. CREATION OF A SOUND FIELD WITH A ZONE OF SILENCE AT THE ORIGIN

A. Theoretical Basis

The solution to the two-dimensional Helmholtz equation at radian frequency ω in polar coordinates $\vec{R} = (R, \phi)$, where $R = \|\vec{R}\|$ and $\phi = \arg\{\vec{R}\}$, may be expressed in the form [21]

$$p(R,\phi,k) = \sum_{m=-\infty}^{\infty} J_m(kR) A_m(k) e^{im\phi}, \tag{1}$$

where $J_m(kR)$ is the cylindrical Bessel function of order *m*, $k = \omega / c$ is the wave number, *c* the speed of sound and $A_m(k)$ is hereafter referred to as the *m*-th order sound field coefficient. For example, for a plane wave arriving from angle ϕ_0, and for a positive time convention $\exp(i\omega t)$, $A_m(k) = i^m e^{-im\phi_0}$.

The expansion in Eq. (1) may be limited to $m \in [-M, M]$ due to the spatial high-pass characteristic of the Bessel functions for $m > 0$. The m-th order Bessel function has a small amplitude for small values of kR and the amplitude becomes significant as kR approaches m, after which it becomes oscillatory in nature, and so for a given kR the order $M = \lceil kR \rceil$, where $\lceil \cdot \rceil$ denotes rounding up to the next highest integer, is often used for an approximated representation of the sound field [22,23].

This property of the Bessel functions also shows how a ZOS may be created at the origin of the coordinate system. If all coefficients up to order $|m| = M_0$ are zero, the sound pressure level for a wave number k will be small over an approximately circular region of radius

$$R_Z \approx \frac{M_0 + 1}{k} \tag{2}$$

centered at the origin. The validity of this formula is demonstrated below. M_0 is hereafter referred to as the zone order. Assume that the coefficients $A_m(k)$ in Eq. (1) are scaled by the high-pass sequence

$$\alpha_m = \begin{cases} 1, |m| > M_0 \\ 0, |m| \le M_0 \end{cases}. \tag{3}$$

The sound pressure is then

$$p_Z(R, \phi, k) = \sum_{m=-\infty}^{\infty} \alpha_m A_m(k) J_m(kR) e^{im\phi}, \tag{4}$$

which will be small over the radius R_Z given by Eq. (2) and generates a ZOS centered at the origin.

As an example, Fig. 1 shows the sound pressure field due to a 1 kHz plane wave arriving from 0 degrees (i.e., from the right), with attenuation of the pressure for radii less than 0.5 m, which correspond to a 9th order ZOS. The magnitude in dB is shown in Fig. 2. The sound level is reduced along the line of propagation (the x-axis) by about 5 dB, with greater attenuation at angles ±9 degrees and 180±9 degrees. The field magnitude at the center of the zone is 0.

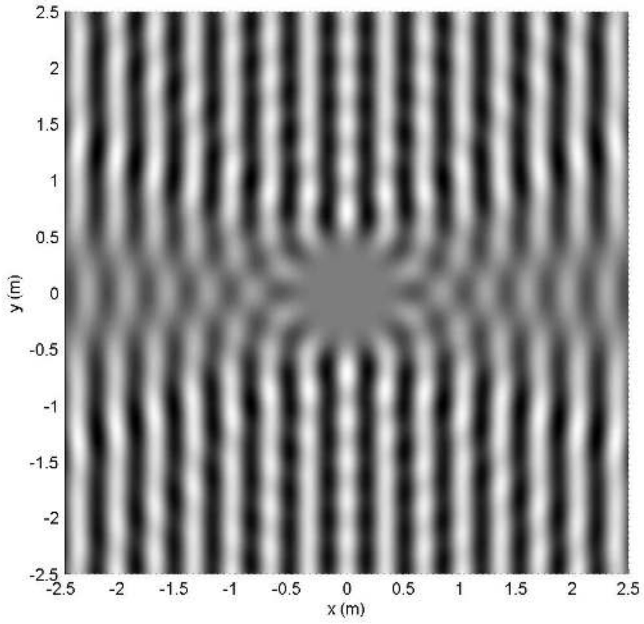

Figure 1: Plane wave with 0.5 m radius ZOS, for a frequency of f = 1 kHz.

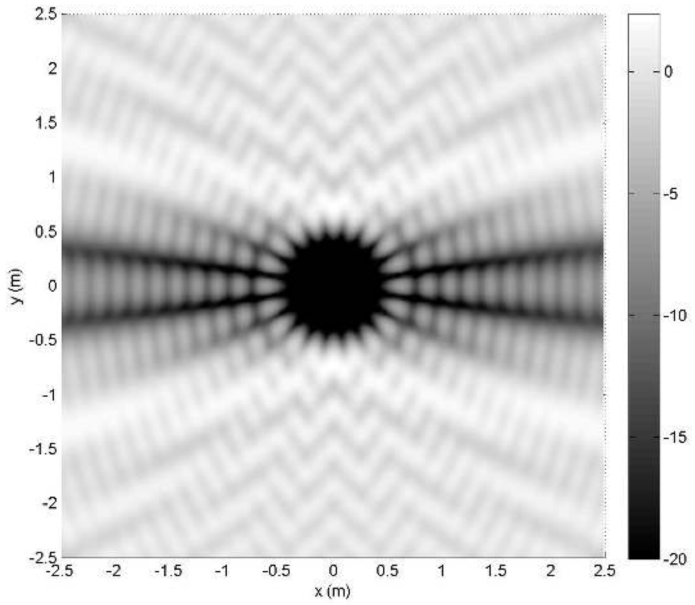

Figure 2: Plane wave with 0.5 m radius null, f = 1 kHz, magnitude in dB.

The sound field obtained using the complementary spatial low-pass sequence to Eq. (3)

$$\beta_m = 1 - \alpha_m = \begin{cases} 0, |m| > M_0 \\ 1, |m| \le M_0 \end{cases}, \tag{5}$$

i.e. the complementary field, may also be defined as

$$p_C(R,\phi,k)=\sum_{m=-\infty}^{\infty}\beta_m A_m(k)J_m(kR)e^{im\phi}=\sum_{m=-M_0}^{M_0}A_m(k)J_m(kR)e^{im\phi}. \tag{6}$$

This sound field tends to be confined within the circular region of radius R_Z, outside of which the acoustic energy decays. The sound field with ZOS can then be written

$$p_Z(R,\phi,k)=p(R,\phi,k)-p_C(R,\phi,k). \tag{7}$$

The average radial level variation, $L_Z(R,k)$, of the ZOS field $p_Z(R,\phi,k)$ can be found by calculating the angle-averaged squared sound pressure from Eq. (4)

$$\left|\overline{p}_Z(R,k)\right|^2=\frac{1}{2\pi}\int_0^{2\pi}\left|p_Z(R,\phi,k)\right|^2 d\phi=\sum_{m=-\infty}^{\infty}\alpha_m^2\left|A_m(k)\right|^2 J_m^2(kR), \tag{8}$$

from which $L_Z(R,k)=10\log_{10}\left(\left|\overline{p}_Z(R,k)\right|^2\right)$. The radial level variation of the complementary field $p_C(R,\phi,k)$ can be found in the same way.

For a plane wave sound field, Eq. (8) yields

$$\left|\overline{p}_Z(R,k)\right|^2=1-\sum_{m=-M_0}^{M_0}J_m^2(kR), \tag{9}$$

which is the truncation error for constructing the approximation to the plane wave using the complementary field in Eq. (6) [23]. A similar expression exists for the 3D case in terms of spherical Bessel functions [23].

An alternative definition of the ZOS radius can be derived from Eq. (8) by noting that for zone order M_0 the sound level for small kR is dominated by the (M_0+1)-th Bessel function. Using the small argument approximation $J_m(x)\approx x^m/(2^m m!)$ the radius where the level has fallen to $20\log_{10}(\gamma)$, for attenuation factor γ, is

$$R_{Z\gamma}=\frac{\left(\gamma 2^{M_0+1}(M_0+1)!\right)^{\frac{1}{M_0+1}}}{k}. \tag{10}$$

The radial level variation of the ZOS field is shown in Fig. 3 for radii up to 1 meter for a 1 kHz plane wave and for zone orders M_0 from 0 to 5. The sound pressure reduces to zero at the origin. An exact pressure null cannot be achieved over the entire region, since such a field would not be a solution of the homogeneous Helmholtz equation. However, the sound pressure is small over an extended area. The size of the region of silence increases with the zone order as expected and the rate of reduction of sound level tends to $20(M_0+1)$ dB per decade. The zone radii from Eq. (2) are shown as circles, and those from Eq. (10) for –20 dB attenuation as diamonds. Equation (2) gives a reasonable estimate of the radius below which the sound level reduces, and Eq. (10) gives a reasonable estimate of the radius for a given attenuation, provided that the attenuation is large enough to make the first term approximation correct. The exact attenuation is not determined because Eq. (10) ignores higher order terms in Eq. (8).

The radial level variation of the complementary field is shown in Fig. 4. The rate of attenuation of the field does not increase significantly with order and does not show the same high attenuation as the ZOS case. For example the 5th order field reduces at around 12 dB per decade. The complementary field is not able to produce a sound zone which is completely confined to $R < R_Z$ since the Bessel functions oscillate out to large values of *kR*. This is intuitively obvious as sound cannot be generated in a region of space surrounding the origin if there is an annular region of silence around that region. In practice, the complementary sound field tends to be large along the line of propagation, and therefore the sound field $p_Z(R,\phi,k)$ tends to be attenuated along the line of propagation, as shown in Figures 1 and 2. If the region where a non-zero sound field is desired is along this line, it will receive a reduced sound pressure. This provides a modal explanation for the fact that two zones of silence do not perform as well when they are in line with the direction of propagation of one or both of the desired sound sources [7].

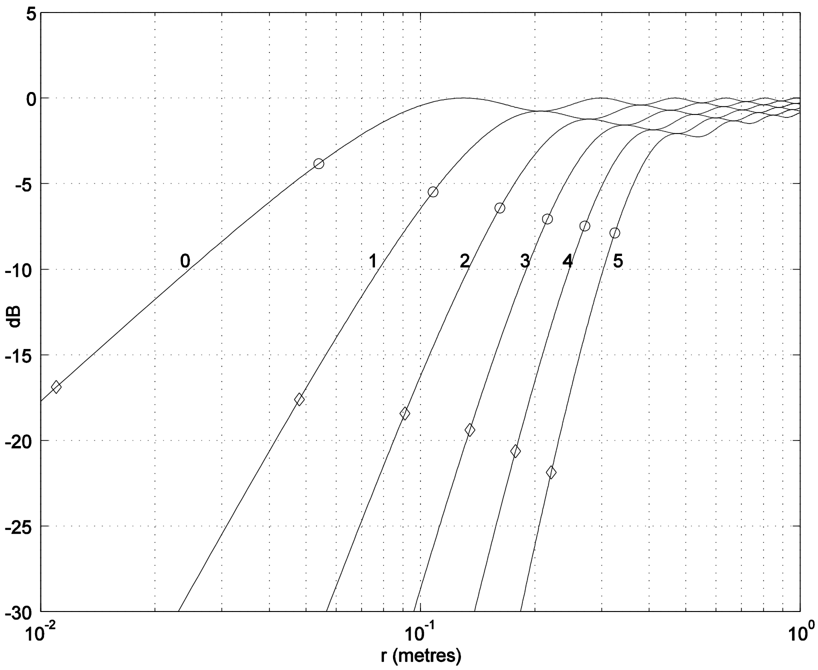

Figure 3: Average radial level variation of ZOS field, for zone orders 0 to 5, *f* = 1 kHz. The zone radii from Eq. (2) are shown as circles and those from Eq. (10) as diamonds.

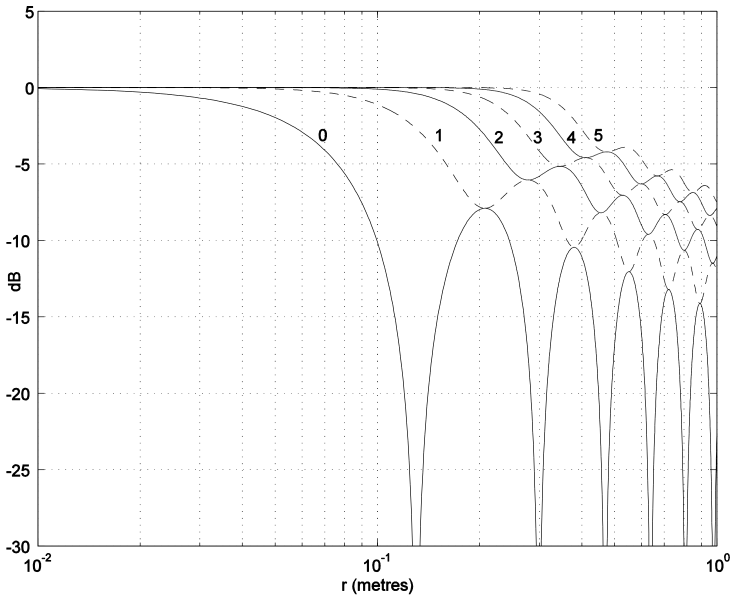

Figure 4: Average radial level variation of complementary field, for zone orders 0 to 5, *f* = 1 kHz. Odd order plots are shown dashed for clarity.

B. Generation of a frequency-invariant zone of silence

The radius of the ZOS for a given order, M_0, is frequency dependent, as per Eq. (2). For the ZOS to be frequency independent, the zone order at each frequency must be

$$M_0(f) = \lceil kR_Z \rceil - 1. \tag{11}$$

The mode suppression sequence α_m becomes a function of frequency, $\alpha_m(f)$ (Fig. 5). In this case the m-th mode is effectively low-pass filtered with a cutoff frequency

$$f(m) = \frac{|m|c}{2\pi R_Z}. \tag{12}$$

The amplitude of the m-th mode for a plane wave at a radius R is $|J_m(kR)|$. For radii less than the zone radius R_Z, the m-th order Bessel function does not become significant for frequencies lower than the mode cutoff frequency and the amplitude of the field generated by that mode is small. For $R > R_Z$ the Bessel function becomes large before the mode cutoff (as shown in Fig. 5) and the magnitude of the field due the sum of modes with $|m| > M_0(f)$ is close to one.

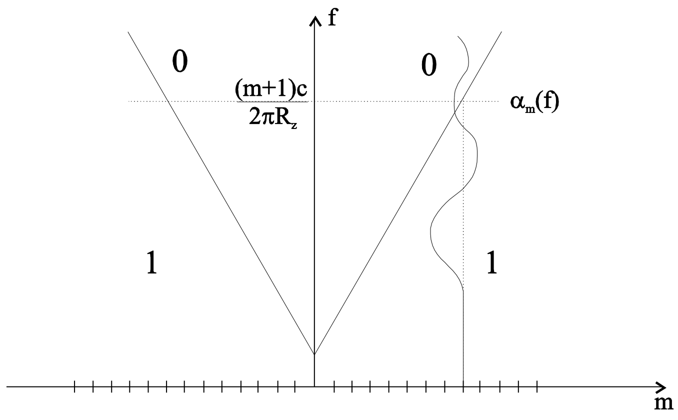

Figure 5: Mode filtering function $\alpha_m(f)$ for a frequency-independent null. The curved line represents schematically the Bessel function of order 8 for $R > R_Z$

The effect of the ideal mode filtering is to produce non-causal solutions in the time domain. Considering the plane wave case for simplicity ($A_m(k) = i^m e^{-im\phi_0}$ which is independent of frequency), the spatial impulse response produced at a field point (R,ϕ) by Eq. (1) when all frequency components have amplitude 1, can be obtained by integrating Eq. (1) with respect to ω, yielding [24]

$$\delta(R,\phi,t) = \begin{cases} \dfrac{c}{\pi R} \displaystyle\sum_{m=-\infty}^{\infty} (-1)^m \frac{\cos\left(m \cos^{-1}(ct/R)\right)}{\sqrt{1-(ct/R)^2}} e^{im(\phi-\phi_0)}, & |t| < R/c \\ 0, & |t| \geq R/c \end{cases}. \tag{13}$$

Each mode produces a signal component of finite duration $|t| < R/c$ which is a weighted Chebyschev polynomial. The sum of these terms produces a delta function at (R,ϕ) which occurs at $\tau = -(R/c)\cos(\phi-\phi_0)$. The impulse response occurs at the negative time $\tau = -R/c$ for $\phi = \phi_0$. In practice any real source at source distance R_s would produce a causal solution due to the additional delay R_s/c to reach the origin.

The effect of the mode filter is to convolve the spatial impulse response with the infinite duration impulse response

$$h_m(t) = \frac{1}{\pi t} \sin\left(\frac{|m|ct}{2\pi R_Z}\right), \tag{14}$$

which is the impulse response of an ideal low-pass filter with cutoff frequency given by Eq. (12). The resulting response cannot be delayed by any amount to produce a causal solution.

This problem is well-known in filter design problems[25]. In practice the low-pass filter can be windowed in time, which produces a finite transition from 1 to zero in the frequency domain. The response may then be delayed to ensure causality. A simple way to achieve this is to produce a linear transition from 0 to 1 above the mode cutoff index in Eq. (11). In the simulations to follow, a linear transition with weights 0, 0.25, 0.5, 0.75 is used for $m = M_0$ to $M_0 + 3$ (with the same behavior for negative m).

III. CREATION OF ZONES OF SILENCE AT ARBITRARY POSITIONS

The theory presented in the previous section allows the generation of frequency-independent nulls positioned at the origin. In order to provide two separate zones with independent sound fields, the null must be positioned at an arbitrary point within a loudspeaker array. This can be done by exploiting an addition property of the cylindrical Bessel function, with reference to Fig. 6.

If a ZOS is positioned at an arbitrary point $\left(R_q, \phi_q\right)$ with local expansion coordinates $\left(R_0, \phi_0\right)$ and corresponding local sound pressure expansion

$$p_q\left(R_0, \phi_0, k\right) = \sum_{n=-\infty}^{\infty} \alpha_n A_n\left(k\right) J_n\left(kR_0\right) e^{in\phi_0} , \tag{15}$$

then the sound field expansion can be expressed in terms of global coordinates $\left(R, \phi\right)$ using the Bessel addition theorem [26]

$$J_n\left(kR_0\right) e^{in\phi_0} = \sum_{m=-\infty}^{\infty} J_m\left(kR\right) e^{im\phi} J_{m-n}\left(kR_q\right) e^{-i(m-n)\phi_q} \tag{16}$$

as

$$p_q\left(R, \phi, k\right) = \sum_{m=-\infty}^{\infty} J_m\left(kR\right) e^{im\phi} \sum_{n=-\infty}^{\infty} \alpha_n A_n\left(k\right) J_{m-n}\left(kR_q\right) e^{-i(m-n)\phi_q} . \tag{17}$$

The global field coefficients, $\hat{A}_m\left(k\right)$, are expressed in terms of the local coefficients, $A_m\left(k\right)$, as

$$\hat{A}_m = \sum_{n=-\infty}^{\infty} \alpha_n A_n\left(k\right) J_{m-n}\left(kR_q\right) e^{-i(m-n)\phi_q} . \tag{18}$$

For example, the sound field produced for a zone positioned at 1 meter from the origin and at an angle of 45 degrees is shown in Fig. 7. The field is identical to that in Fig. 1, but shifted to the zone coordinates.

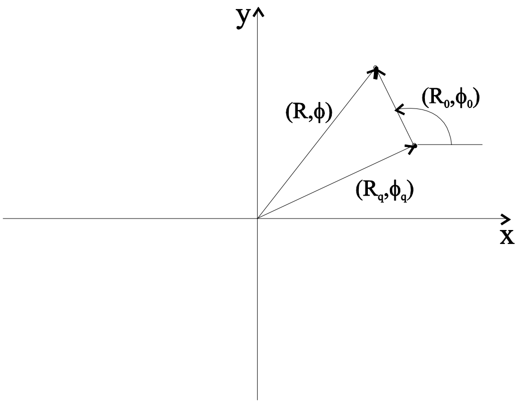

Figure 6: Addition theorem coordinates.

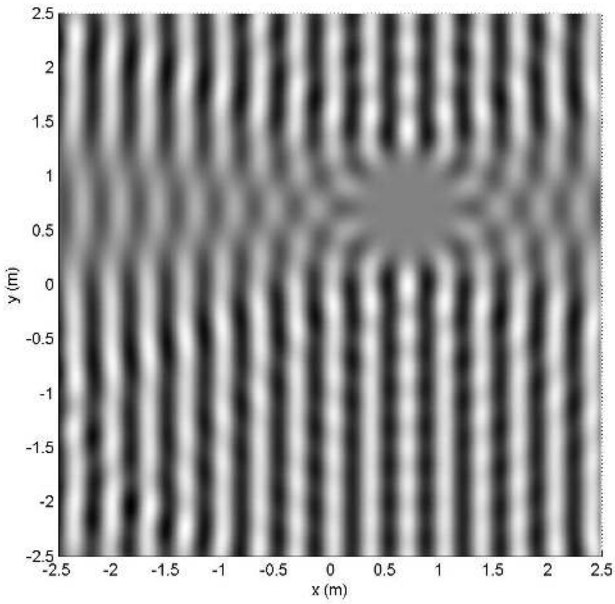

Figure 7: Plane wave with 0.5 m radius null positioned at 1 metre from origin at 45 degrees, for a frequency of *f* = 1 kHz.

IV. GENERATION OF A TWO-ZONE SOUND FIELD USING A DISCRETE ARRAY OF SOURCES

If two sound fields are produced, which have non-overlapping zones of silence positioned at different positions $\left(R_q,\phi_q\right)$, $q=1,2$, then at each ZOS position, only one sound field will be heard, and a two-zone sound field is produced. At positions other than the two null positions, both fields will be heard.

The two sound fields can be produced in practice using a circular array of L sources positioned at radius R_L, with angles $\phi_l = 2\pi l/L, l \in [0, L-1]$. The spatial Nyquist frequency of the array is [27]

$$f_{Nyq} = \frac{c(L-1)}{4\pi R_L} \ . \qquad (19)$$

The array is able to reproduce a desired sound field up to f_{Nyq} for all radii $R \le R_L$.

The required line source weights to produce a sound field with coefficients $\hat{A}_m(k)$ can be determined by first assuming the field is produced by a continuous distribution of sources

$$p(R,\phi,k) = \frac{1}{2\pi}\int_0^{2\pi} H_0\left(k\left|\vec{R}-\vec{R}_L\right|\right) w(\phi_s)\, d\phi_s \ , \qquad (20)$$

where the cylindrical Hankel function is proportional to the 2D free-space Greens function [21] and $w(\phi_S)$ is the source amplitude at angle ϕ_S. The function $H_0\left(k\left|\vec{R}-\vec{R}_L\right|\right)$ may be expressed in global coordinates as [26]

$$H_0\left(k\left|\vec{R}-\vec{R}_L\right|\right) = \sum_{m=-\infty}^{\infty} J_m(kR) H_m(kR_L) e^{im(\phi-\phi_s)} \ . \qquad (21)$$

The source amplitude $w(\phi_S)$ may be expressed as a Fourier expansion

$$w(\phi_s) = \sum_q \varepsilon_q e^{iq\phi_s} \ , \qquad (22)$$

with expansion coefficients ε_q. Substituting Eq.s (21) and (22) into (20) and requiring the result to be of the form of Eq. (1), with sound field coefficients $\hat{A}_m(k)$, yields $\varepsilon_m = \hat{A}_m(k)/H_m(kR_L)$. Sampling the solution at the discrete source angles ϕ_l, for a maximum mode order $M = (L-1)/2$, produces the discrete source weights [27]

$$w_l = \frac{1}{L}\sum_{m=-M}^{M} \frac{\hat{A}_m(k) e^{im\phi_l}}{H_m(kR_L)} . \qquad (23)$$

Let $\hat{B}_m(k)$ and $\hat{D}_m(k)$ be the set of coefficients describing the two independent null fields associated with the two zones. The coefficients $\hat{A}_m(k)$ describing the sound field generated by the linear superposition of the two null fields are given by

$$\hat{A}_m(k) = \hat{B}_m(k) + \hat{D}_m(k) . \qquad (24)$$

Inserting these coefficients in Eq. (23), a two-zone sound field may be produced.

As an example, we consider a circular array of 351 sources at a radius of 2 m, producing a spatial Nyquist frequency of 4.7 kHz. We generate two sound fields, each being a pulse of bandwidth 4 kHz and each producing a ZOS at a distance of 1 m from the origin, with one zone at an angle of 0 degrees (zone to the right in the figure) and the other at 180 degrees. In the first zone a pulse arriving from an angle of 135 degrees (from top-left of the figure) will be produced and in the second zone a pulse arriving from 45 degrees (from top-right) will be produced.

The sound field was calculated at 100 frequencies up to 4 kHz, with a time duration of 25 ms (and a delay of 12.5 ms to ensure causality). Figure 8 shows the individual sound fields at 12.5 ms, when each pulse is crossing its corresponding ZOS.

Figure 9 shows the pulses at 18.4 ms, when they are crossing their corresponding target zones. The pulses are accurately produced in the target zones.

If the angle of arrival of the pulse is in line with the two zone centers, then the pulse reproduced in the target zone will be reduced in amplitude, since the wave front must avoid the ZOS. This is shown in Fig. 10 for a single pulse arriving from zero degrees angle of incidence. Fig 10(a) shows the sound field when the pulse is crossing the null region and Fig. 10(b) shows the pulse at the center of the desired zone. The wave front produced in the desired zone has artefacts caused by the residual diffraction of sound around the null zone.

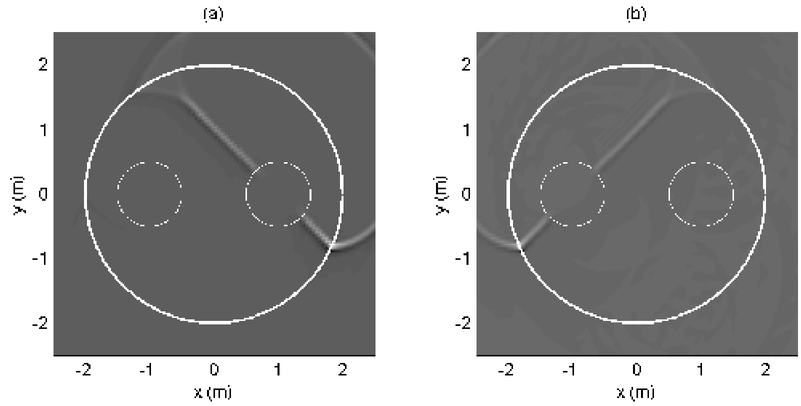

Figure 8: Sound fields due for two zones at 1 metre radius with 4 kHz bandwidth pulses arriving from 45 degrees (a) and 135 degrees (b), at t = 12.5 ms.

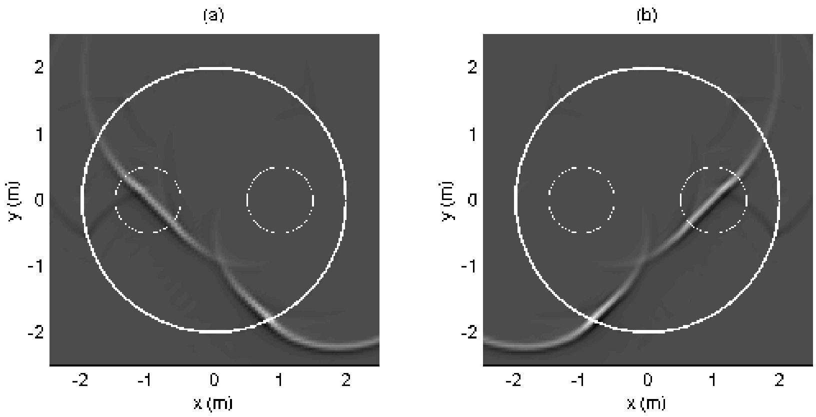

Figure 9: Sound fields due for two zones at 1 metre radius with 4 kHz bandwidth pulses arriving from 45 degrees (a) and 135 degrees (b), at *t* = 16.7 ms.

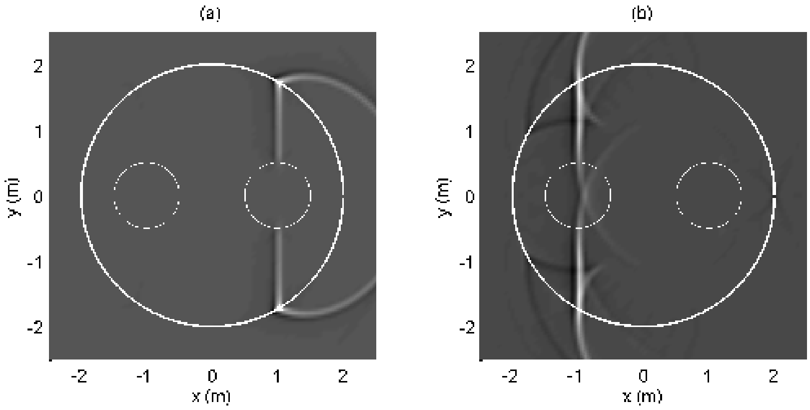

Figure 10: Sound fields due for two zones at 1 metre radius with a 4 kHz bandwidth pulse arriving from 0 degrees, at *t* = 12.5 ms (a) and at t = 18.4 ms (b).

V. CONCLUSIONS

This paper has provided a theoretical basis for the generation of a single zone of silence, based on the elimination of low order modes in the cylindrical expansion of the sound field. Frequency-invariant nulls can be produced by suppressing increasing numbers of modes with increasing frequency. It has been shown that broadband pulses can be synthesized that avoid the zone of silence.

While the theory has been restricted to 2D for simplicity, similar results occur in the 3D case. For example the angle-averaged sound pressures for a plane wave and given zone order have similar forms to Fig. 3 for the 3D case and the zone pressure can be calculated in terms of spherical Bessel functions[23]. However, the generation of 3D fields requires considerably more sources than the 2D case and is less likely to be implemented. While a circular array of ideal line sources has been used for the 2D simulations presented here, zones of silence with similar behavior are also produced if the line sources are replaced with point sources and the sectorial approximation used [28], but this has not been considered here.

The generation of a single ZOS provides a way to produce two sound zones using the same loudspeaker array, where different program material is heard in each zone. The advantage of the method presented here is that significant suppression of the sound pressure is produced in the target null zone, provided that the loudspeakers are well-matched. However, the ZOS is produced at the expense of some distortion of the wave field in the other zone, particularly when it is in line with the direction of propagation of the sound.

The ZOS technique creates two global sound fields within a speaker array, each with a small local null. This contrasts with the spatial bandstop approach which creates local zones using lower order modes in each zone, and cancels the residual effect of these local modes in a second zone using higher order modes which have small amplitudes in the first zone [13].

The theory presented here shows that the production of a two-zone personal sound system is well-founded. However, it offers little support for the generation of three or more zones. Previous publications have shown that three zones can be produced, and it is clear that well-separated zones can have independent sound fields via beam forming techniques. Hence the theory presented here is applicable to the two-zone problem only, and does not preclude the generation of higher numbers of zones.

This paper has assumed free-field conditions. The creation of a zone of silence in a reverberant room would produce zero direct field within the zone, but room reflections would be produced within the zone, destroying the independence of the sound fields in the two zones. However, the use of active cancellation of reverberation would allow zones of silence to be produced in the reverberant case [29]. The control of higher order modes means that the region of cancellation can be larger than obtained by zeroth-order pressure control, which produces a region of around one tenth of a wavelength [30].

[1] W.F. Druyvesteyn and J. Garas, "Personal Sound," J. Audio Eng. Soc. **45**, 685–701 (1997).

[2] J.-W. Choi and Y.-H. Kim, "Generation of an acoustically bright zone with an illuminated region using multiple sources," J. Acoust. Soc. Am. **111**, 1695–1700 (2002).

[3] J.-W. Choi and Y.-H. Kim, "Manipulation of sound intensity within a selected region using multiple sources," J. Acoust. Soc. Am. **116**, 843–852 (2004).

[4] M. Jones and S.J. Elliott, "Personal audio with multiple dark zones," J. Acoust. Soc. Am. **124**, 3497–3506 (2008).

[5] T.D. Abhayapala and Y.J. Wu, "Spatial soundfield reproduction with zones of quiet," AES 127th Convention (2009).

[6] Y.J. Wu and T.D. Abhayapala, "Spatial Multizone Soundfield Reproduction: Theory and Design," IEEE Trans. Audio, Speech Lang. Proc. **19**, 1711–1720 (2011).

[7] M.A. Poletti, "An Investigation of 2D Multizone Surround Sound Systems," AES 125th Convention (2008).

[8] J. Chang, C.-H. Lee, J.-Y. Park, and Y.-H. Kim, "A realization of sound focused personal audio system using acoustic contrast control," J. Acoust. Soc. Am. **125**, 2091–2097 (2009).

[9] J.-Y. Park, J.-H. Chang, and Y.-H. Kim, "Generation of independent bright zones for a two-channel private audio system," J. Audio Eng. Soc. **58**, 382–393 (2010).

[10] J.-H. Chang, J.-Y. Park, and Y.-H. Kim, "Scattering effect on the sound focused personal audio system," J. Acoust. Soc. Am. **125**, 3060–3066 (2009).

[11] M. Shin, S.Q. Lee, F.M. Fazi, P.A. Nelson, D. Kim, S. Wang, K. ho Park, and J. Seo, "Maximization of acoustic energy difference between two spaces," J. Acoust. Soc. Am. **128**, 121–131 (2010).

[12] N. Radmanesh and I.S. Burnet, "Generation of isolated wideband sound fields using a combined two-stage lasso-LS algorithm," IEEE Trans. Audio, Speech Lang. Proc. **21**, 378–387 (2013).

[13] Y.J. Wu and T.D. Abhayapala, "Multizone 2D soundfield reproduction via spatial band stop filters," IEEE Workshop on Applications of Signal Processing to Audio and Acoustics (2009).

[14] Y. Cai, M. Wu, and J. Yang, "Sound reproduction in personal audio systems using the least-squares approach with acoustic contrast control constraint," J. Acoust. Soc. Am. **135**, 734–741 (2014).

[15] J. Chang and F. Jacobsen, "Sound field control with a circular double-layer array of loudspeakers," J. Acoust. Soc. Am. **131**, 4518–4525 (n.d.).

[16] P. Coleman, P. Jackson, M. Olik, and J.A. Pedersen, "Optimizing the planarity of sound zones," AES 52nd Intl. Conf. (2013).

[17] W. Jin, W.B. Kleijn, and D. Virette, "Multizone soundfield reproduction using orthogonal basis expansion," Intl. Conf. Acoust. Speech Sig. Proc. (ICASSP) 311–315 (2013).

[18] W. Jin and W.B. Kleijn, "Multizone soundfield reproduction in reverberant rooms using compressed sensing techniques," Intl. Conf. Acoust. Speech Sig. Proc. (ICASSP) (2014).

[19] D.I. Havelock and A.J. Brammer, "Directional loudspeakers using sound beams," J. Audio Eng. Soc. **48**, 908–916 (2000).

[20] S. Baek, M.-S. Song, S.-P. Lee, and H.-G. Kang, "Speaker array system based on equalization method with a quiet zone," 127th AES Conv. (2009).

[21] E.G. Williams, *Fourier Acoustics* (Academic Press, San Diego, CA, 1999), pp. 115–234.

[22] R.A. Kennedy, P. Sadeghi, T.D. Abhayapala, and H. Jones, "Intrinsic limits of dimensionality and richness in random multipath fields," IEEE Trans. Signal Proc. **55**, 2542–2556 (2007).

[23] D.B. Ward and T.D. Abhayapala, "Reproduction of a plane-wave sound field using an array of loudspeakers," IEEE Trans. Speech and Audio Processing **9**, 697 – 707 (2001).

[24] M.A. Poletti, "A Unified Theory of Horizontal Holographic Sound Systems," J. Audio Eng. Soc. **48**, 1155–1182 (2000).

[25] A. V. Oppenheim and R.W. Schafer, *Digital Signal Processing*, 1st ed. (Prentice-Hall, Englewood Cliffs, New Jersey, 1975), pp. 237–271.

[26] G.N. Watson, *A Treatise on the Theory of Bessel Functions*, 2nd ed. (Cambridge Univ. Press, New York, NY, 1995), p. Chap. 7, 198.

[27] M.A. Poletti and T.D. Abhayapala, "Interior and exterior sound field control using general two-dimensional first-order sources.," J. Acoust. Soc. Am. **129**, 234–244 (2011).

[28] J. Ahrens and S. Spors, "An analytical approach to sound field reproduction using circular and spherical loudspeaker distributions," Acta Acustica united with Acustica **94**, 988–999 (2008).

[29] T. Betlehem and M.A. Poletti, "Two dimensional sound field reproduction using higher order sources to exploit room reflections," J. Acoust. Soc. Am. **135**, 1820–1833 (2014).

[30] S.J. Elliott, P. Joseph, A.J. Bullmore, and P.A. Nelson, "Active cancellation at a point in a pure tone diffuse sound field," J. Sound Vib. **120**, 183–189 (1988).

Figure Captions

Figure 1: Plane wave with 0.5 m radius ZOS, for a frequency of $f = 1$ kHz.

Figure 2: Plane wave with 0.5 m radius null, $f = 1$ kHz, magnitude in dB.

Figure 3: Average radial level variation of ZOS field, for zone orders 0 to 5, $f = 1$ kHz. The zone radii from Eq. (2) are shown as circles and those from Eq. (10) as diamonds.

Figure 4: Average radial level variation of complementary field, for zone orders 0 to 5, $f = 1$ kHz. Odd order plots are shown dashed for clarity.

Figure 5: Mode filtering function $\alpha_m(f)$ for a frequency-independent null. The curved line represents schematically the Bessel function of order 8 for $R > R_Z$.

Figure 6: Addition theorem coordinates.

Figure 7: Plane wave with 0.5 m radius null positioned at 1 meter from origin at 45 degrees, for a frequency of $f = 1$ kHz.

Figure 8: Sound fields due for two zones at 1 meter radius with 4 kHz bandwidth pulses arriving from 45 degrees (a) and 135 degrees (b), at $t = 12.5$ ms.

Figure 9: Sound fields due for two zones at 1 meter radius with 4 kHz bandwidth pulses arriving from 45 degrees (a) and 135 degrees (b), at $t = 16.7$ ms.

Figure 10: Sound fields due for two zones at 1 meter radius with a 4 kHz bandwidth pulse arriving from 0 degrees, at $t = 12.5$ ms (a) and at $t = 18.4$ ms (b).